



## Testing regional vertical total electron content maps over Europe during the 17–21 January 2005 sudden space weather event

R. Orus,<sup>1,3</sup> L. R. Cander,<sup>2</sup> and M. Hernandez-Pajares<sup>3</sup>

Received 28 April 2006; revised 5 December 2006; accepted 15 January 2007; published 12 May 2007.

[1] The intense level of solar activity recorded from 16 to 23 January 2005 led to a series of events with different signatures at the Earth's ionospheric distances. Measurements of the critical frequency of the  $F_2$  layer  $f_oF_2$  and the vertical total electron content (VTEC) are used to describe the temporal and spatial electron density distributions during this space weather event, which gives an excellent opportunity to test regional VTEC maps over Europe under such disturbed solar-terrestrial conditions. In this context, the tests used to validate the International GNSS Service (IGS) VTEC maps have been applied to assess the accuracy of the European Rutherford Appleton Laboratory (RAL) VTEC maps. Thus the self-consistency test and the Jason altimeter test have been used to compare such performances with the IGS and Universitat Politècnica de Catalunya global ionospheric maps. The results show discrepancies between the RAL maps and the IGS ones, which leads to significant RMS and bias values of several total electron content units. Moreover, in this work a kriging technique to improve the accuracy of any regional VTEC map is also considered, with relative improvements of the RAL VTEC maps up to more than 20% at the peak of the storm.

**Citation:** Orus, R., L. R. Cander, and M. Hernandez-Pajares (2007), Testing regional vertical total electron content maps over Europe during the 17–21 January 2005 sudden space weather event, *Radio Sci.*, 42, RS3004, doi:10.1029/2006RS003515.

### 1. Introduction

[2] The ionospheric response to the complex changes in solar wind, magnetosphere and thermosphere conditions during sudden severe space weather events, in particular the “Halloween storms” of 29–30 October 2003 has recently been the subject of a number of different studies [e.g., Liu and Lühr, 2005; Mannucci et al., 2005; Meier et al., 2005; Cander and Mihajlovic, 2005; Hernández-Pajares et al., 2005]. They all show that the current capability to provide ionospheric space weather measurements, reasonably accurate forecasts of

ionospheric conditions and timely alert warnings is limited by current ionospheric sensing facilities, density and frequency of ionospheric measurements and accuracy of ionospheric models. A significant improvement of the ionospheric space weather support for different applications requires our ability to frequently measure the ionosphere vertically and horizontally. It is well known that to achieve this enhancement daily, consistent in time and space, an accurate worldwide and/or regional ionospheric mapping capability is required.

[3] In this framework, the use of different systems, as for example ionosonde data and GPS data, can be suitable in order to describe the ionospheric behavior in such stormy conditions. The ionosonde data can give an accurate vertical description of the ionosphere. However, as the number of ionosonde stations in the European area is limited, it could lead to very big horizontal data gaps. Under these circumstances the GPS system has shown to be an excellent tool when it is necessary to compute maps of vertical ionospheric total electron content (TEC). This is due to the fact that different worldwide or regional dense GPS networks exist, such as the International GNSS Service (IGS) [see Beutler

<sup>1</sup>Wave Interaction and Propagation Section, European Space Research and Technology Centre, European Space Agency, Noordwijk, Netherlands.

<sup>2</sup>Rutherford Appleton Laboratory, Chilton, UK.

<sup>3</sup>Research Group of Astronomy and Geomatics, Universitat Politècnica de Catalunya, Barcelona, Spain.

**Table 1.**  $A_p$  and  $K_p$  Values for the Week 15–21 January 2005

Date	$A_p$ (3 hours)	$K_p$ (3 hours)
15 Jan 2005	22	3, 6, 4, 3, 3, 3, 3, 2
16 Jan 2005	12	2, 2, 2, 2, 3, 3, 2, 3
17 Jan 2005	63	5, 4, 3, 7, 7, 7, 5, 3
18 Jan 2005	72	6, 5, 7, 5, 6, 6, 4, 5
19 Jan 2005	62	6, 6, 6, 7, 6, 4, 3, 4
20 Jan 2005	12	2, 1, 1, 2, 4, 4, 3, 3
21 Jan 2005	61	3, 1, 3, 2, 2, 8, 8, 6

*et al.*, 1999] receivers (worldwide distributed) or the European Reference Frame (EUREF) network (with more than 100 stations distributed across the European region). Thus there are different approaches in order to obtain an accurate ionospheric mapping determination, such as regional ionospheric mapping techniques [Cander *et al.*, 2003; Jakowski, 1998], which allow near real time ionospheric determination, or the global ionospheric maps (GIMs) computed in postprocess by the IGS (see Feltens and Schaer [1998] for details).

[4] This paper is concerned with the ionospheric consequences of the 17–21 January 2005 sudden space weather events. We first analyze the measurements of the critical frequency of the ionospheric  $F_2$  layer  $f_oF_2$  from a European network of ground-based ionosondes and the vertical total electron content (VTEC) derived from the European network of Global Positioning System (GPS) ground-based receivers in order to identify the overall spatial and temporal pattern of  $f_oF_2$  and VTEC behavior over Europe (section 2). In section 3, two possible methods of the regional map testing are presented. Then, the results of testing VTEC Rutherford Appleton Laboratory (RAL) regional maps over Europe [Cander *et al.*, 2003] and the IGS VTEC maps are shown in such high geomagnetic conditions. In this context, the different VTEC maps are compatible between them at 1 total electron content units (TECU) level in standard deviation but at 2 TECU level in bias regarding to the Jason-1 VTEC estimation. Moreover, in section 4, a method to improve the regional VTEC maps, based in the kriging mapping technique, is shown jointly with the use of the “leveled” carrier phase obtained from computing the ambiguity term with the ionospheric map. Thus this method shows relative improvements up to more than 20% when the RAL ionospheric maps are used.

## 2. The 20 January 2005 Sudden Space Weather Event

[5] The whole week from 16 January 2005 was dominated by one single big sunspot group, which was clearly visible on the solar disk (<http://sidc.oma.be>)

[see, e.g., Garcia-Rigo *et al.*, 2007]. The group produced an M- and X-flaring period with a wide impact on both solar-terrestrial physical system and technology. Together with the flares and associated interplanetary coronal mass ejections (ICMEs), several proton events occurred. On 16 January around 0930 UT, ACE data showed changing in several physical quantities: higher density, decreasing temperature, high solar wind speed, increased total interplanetary magnetic field. A clear shock was seen in ACE data on 17 January at 0700 UT when the solar wind speed changed from slightly beneath 600 up to 650 km/s. Then at 1030 UT the speed rose more smoothly to 800 km/s. The total interplanetary magnetic field  $B_t$  went up to 40 nT, while its  $B_z$  component reached  $-20$  nT. This was the onset of a severe geomagnetic storm with  $K_p$  up to 7 on 17 January; see Table 1 to see the  $K_p$  and  $A_p$  values during the storm period.

[6] The night between 17 and 18 January sees several changes in  $B_t$  and  $B_z$  and the solar wind speed reaches 1000 km/s at the beginning of 19 January, resulting in two days of severe geomagnetic disturbances on 18 and 19 January. Although the next day ACE showed some evidence for another CME passing through, it was not until the solar wind speed made a sudden jump from 600 up to 1000 km/s and  $B_z$  went down to more than  $-20$  nT around 1650 UT on 21 January that a sudden severe geomagnetic storm with  $K_p$  equal to 8 occurred.

[7] The ionospheric density and composition experience significant changes both globally and locally during these geomagnetic storms. The electron density disturbances in the ionospheric  $F$  region during 16–23 January 2005 as measured at the Chilton ionospheric station ( $51.6^\circ\text{N}$ ,  $358.7^\circ\text{E}$ ) are shown in Figure 1a. The quiet time reference value for this storm was the monthly median for January 2005. Using an hourly ionospheric activity index  $\text{AI}(f_oF_2)$  that is the percentage difference  $(f_oF_2^{\text{storm}} - f_oF_2^{\text{median}})/f_oF_2^{\text{median}}$  to express the density deviation from quiet time values (see results in Figure 1b). On the dayside, strong density enhancements of  $\sim 40\%$  occurred around 1100 on 17 January, which is clearly distinguished from the monthly median data. The daytime density enhancement reached another maximum of more than 50% during daytime on 18 January, before a negative storm phase of almost 3 days duration has developed. A small density enhancement of  $\sim 30\%$  appeared again around 1800 UT on 21 January, corresponding to the occurrence of the second geomagnetic storm.

[8] The response of the vertical total electron content VTEC derived from the GPS receiver (see Cander and Ciraolo [2002] for details of the technique) at Hailsham ( $50.9^\circ\text{N}$ ,  $0.3^\circ\text{E}$ ), near to Chilton ionosonde station, to changes in geomagnetic activity during the period 16–23 January 2005 shown in Figure 2 is very similar to the

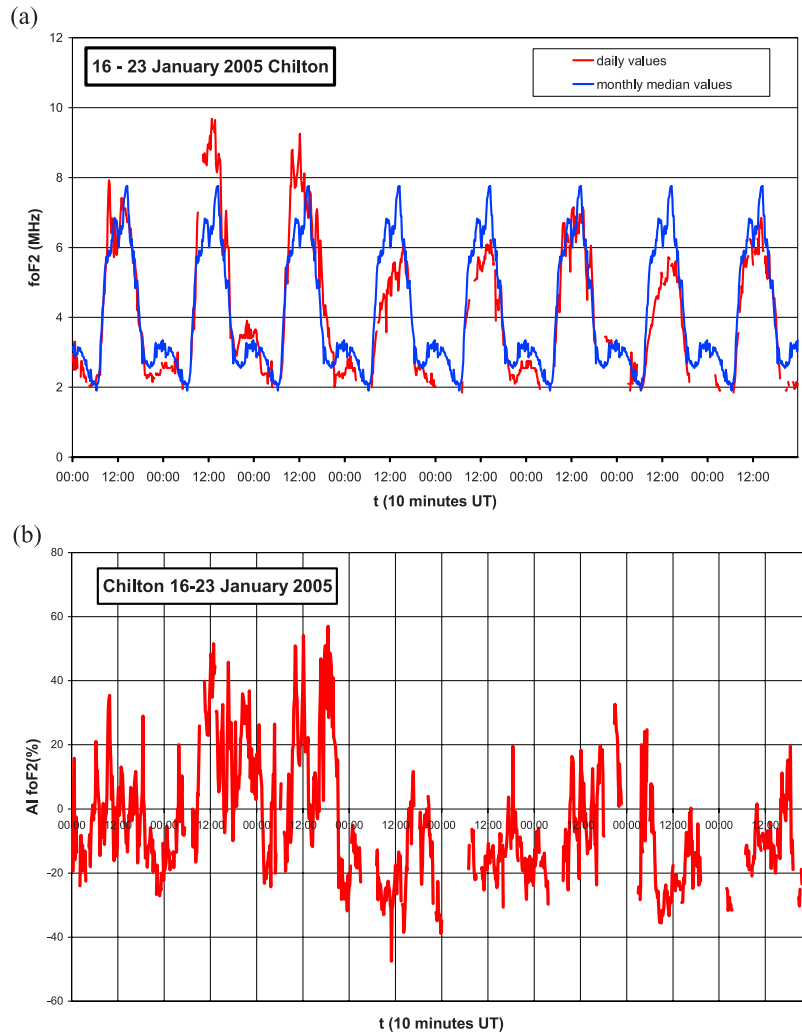


**Figure 1.** (a) Hourly  $f_oF_2$  values measured at the Chilton ionospheric station ( $51.6^\circ\text{N}$ ,  $358.7^\circ\text{E}$ ) together with  $f_oF_2$  January monthly medians. (b) Hourly ionospheric activity index expressing the relative intensity of the disturbance in percentage terms.

$f_oF_2$  responses as seen in Figure 1. Two strong density enhancements can be clearly recognized during daytime of both 17 and 18 January 2005. The observed TEC increases of  $\sim 100\%$ – $170\%$  on the first day are correlated with enhanced  $B_z$ . The negative phase of the storm is most pronounced on 20 January.

[9] Variability of  $f_oF_2$  with space is shown in Figure 3 by plotting hourly  $f_oF_2$  values measured at five ionospheric stations in Europe during 17–19 January 2005. During this period the first geomagnetic storm created ionization disturbances that were predominantly positive at all stations on 17 January. Significant ionization

depletion in  $f_oF_2$  at Juliusruh occurred on 18 January, when a similar negative storm effect in  $f_oF_2$  only started to appear at Pruhonice and Chilton. It is evident that the storm did not produce a similar negative effect at stations around  $40^\circ\text{N}$  Tortosa and El Arenosillo even on 19 January when the negative storm developed fully at three stations at latitudes  $>50^\circ\text{N}$ .

[10] The ionosonde measurements were then compared to VTEC data obtained from a few European IGS GPS receivers. Typical derived VTEC [see *Cander and Ciruolo, 2002*] displaying the evaluation of the 10 min vertical TEC values from observation on 16–23 January

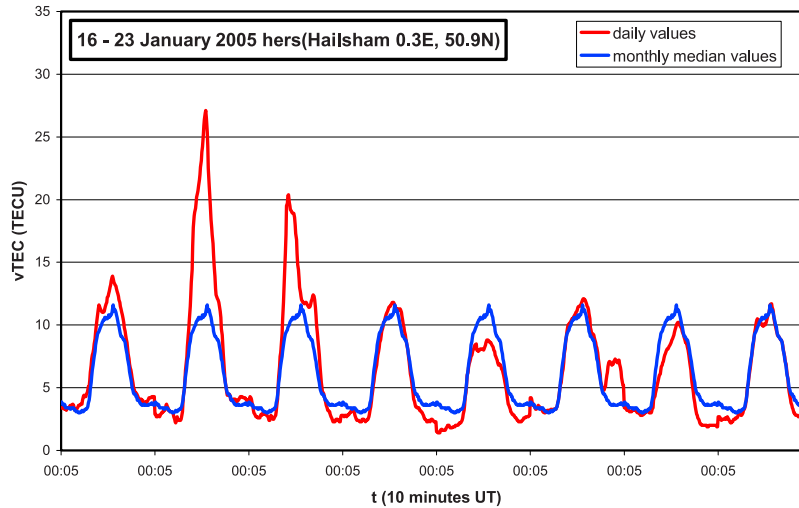


**Figure 2.** The 10 min VTEC values at the Hailsham GPS receiver (50.9°N, 0.3°E) together with VTEC January monthly medians.

2005 (see results in Figure 4). It can easily be seen that the total ionospheric content was highly disturbed both in time and in space over the European area. As expected, the positive ionospheric storm is detected from midday 17 January to late night on 18 January at all sites but not ARTI. Figure 4 shows VTEC depletions of different scale relative to the TEC values on the quiet ionospheric day that are observed at all sites after 18 January. The observed structures in the ionospheric/plasmaspheric ionization with some common  $f_oF_2$  and VTEC features

as well as distinctly different irregularities during this space weather event display behavior even within such a limited area.

### 3. Methods and Results of Testing VTEC Regional Maps Over Europe

[11] As has been mentioned above, the methods used to test VTEC regional maps are those used for IGS ionospheric working group to validate their global iono-

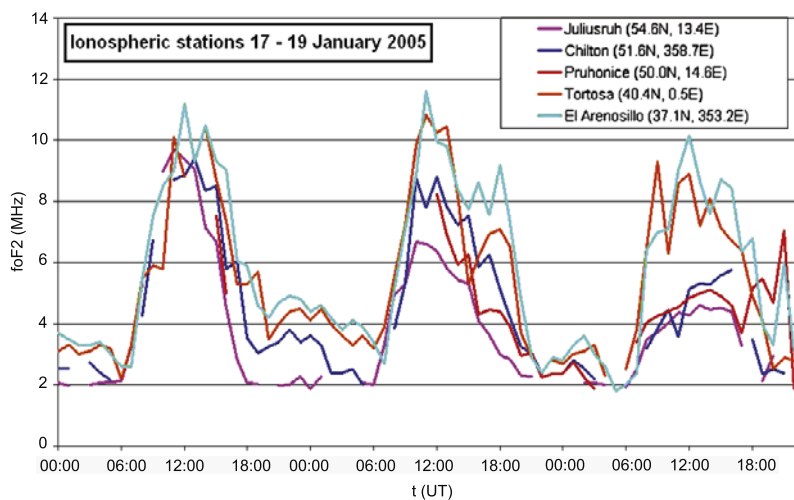


**Figure 3.** Hourly  $f_oF_2$  values measured at five ionospheric stations in Europe during 17–19 January 2005.

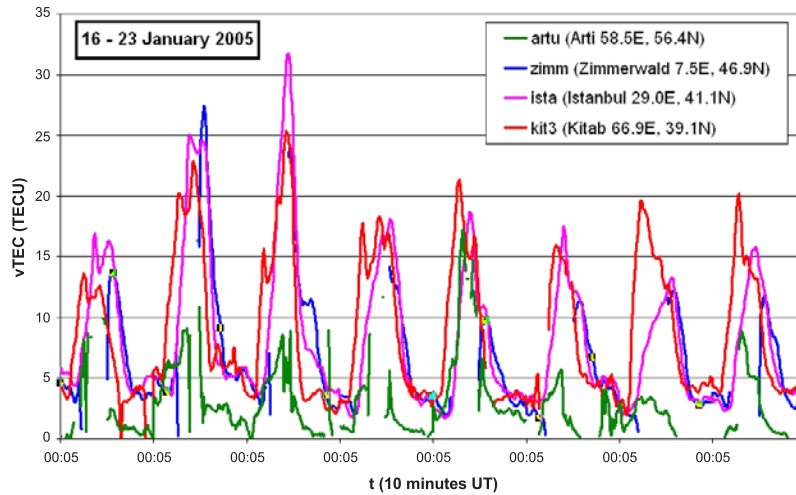


**Figure 4.** The 10 min VTEC values at four GPS receivers in Europe during 16–23 January 2005.

spheric maps (GIMs) (<http://igs.cb.jpl.nasa.gov>). Thus the self-consistency test (which uses the GPS carrier phase data) and the Jason altimeter test (which employs the derived Jason-1 dual frequency altimeter ionospheric data) are adapted, as will be explained in this section, to perform the regional validation.

[12] The Rutherford Appleton Laboratory (RAL), United Kingdom, provides an interactive continuous service for short-term ionospheric forecasting (STIF) at <http://ionosphere.rcru.rl.ac.uk/>. Part of this service, related to the EU COST271 action [Zolesi, 2004], is regional TEC maps. The derived VTEC values are computed using the method developed by *Ciraolo and Spalla* [1997].

[13] On the other hand, since 1 June 1998 the IGS ionospheric working group is computing GIM with GPS data [see *Feltens and Schaer*, 1998], and it started to deliver an official IGS GIM on May 2003 on the Web site <ftp://cddis.gsfc.nasa.gov/gps/products/ionex>, which is the combination of the individual GIM computed by the University of Berne (CODE), European Space Agency (ESA), Jet Propulsion Laboratory (JPL) and Universitat Politècnica de Catalunya (UPC). In previous studies (see *Orus et al.* [2003] for details), the accuracy of such GIMs was assessed for the year 2000, showing that the most accurate GIMs had a relative error of about 12%, relative to TOPEX altimeter data, in the Mediterranean Sea. This result makes them suitable to have a reference for the VTEC ionospheric maps. It has to be pointed out that the sampling time of the IGS GIMs is 2 hours in front of the 10 min of the RAL VTEC maps. This feature is important since when the TEC values have to be computed for any time, the two nearest VTEC maps in time are linearly interpolated in approximately sun fixed reference frame [see *Feltens and Schaer*, 1998].

### 3.1. Self-Consistency Test

[14] The self-consistency test (see *Orus et al.* [2005] for details) is employed by the IGS ionospheric working group in order to validate the different IGS GIMs computed from GPS data and to assign the individual weights to compute the combined IGS GIM. This test measures the capability of a certain model to reproduce the differences of the ionospheric carrier phase observable ( $L_I$ ) over a single station as a function of the elevation of the satellites in view. Such differences are done guaranteeing a minimum time span between consecutive samples, in such a way that just rising and setting up satellite observations, with the same elevations and without any intermediate cycle slip (i.e., within a continuous arch of carrier phase measurements) are involved. In fact, it is a measure of difference of the slant TEC (STEC), computed from the VTEC map as described by *Feltens and Schaer* [1998], at two different epochs in a continuous carrier phase arc. Thus, with this difference, the ambiguity term ( $B_I$ ) of the observed carrier phase data is removed, providing an ionospheric reference value better than one tenth of TECU. Thus the RMS ( $RMS_{\text{self}}$ ) of this test can be computed as follows:

$$RMS_{\text{self}} = RMS[L_I(\varepsilon_{t1}) - STEC_{\text{Model}}(\varepsilon_{t1}) - (L_I(\varepsilon_{t2}) - STEC_{\text{Model}}(\varepsilon_{t2}))] \quad (1)$$

where  $L_I$  is the ionospheric geometry-free combination of GPS carrier phases; the STEC is the slant TEC of the different ionospheric models;  $RMS_{\text{self}}$  is the RMS of the difference among the  $L_I$  observations and the STEC predictions at the same elevation  $\varepsilon$  in a continuous arc taking this difference at two different times, for instance,  $t_1$  and  $t_2$ .

[15] Thus the test proposed in this work is based on the estimation of the different  $RMS_{\text{self}}$  over nine European

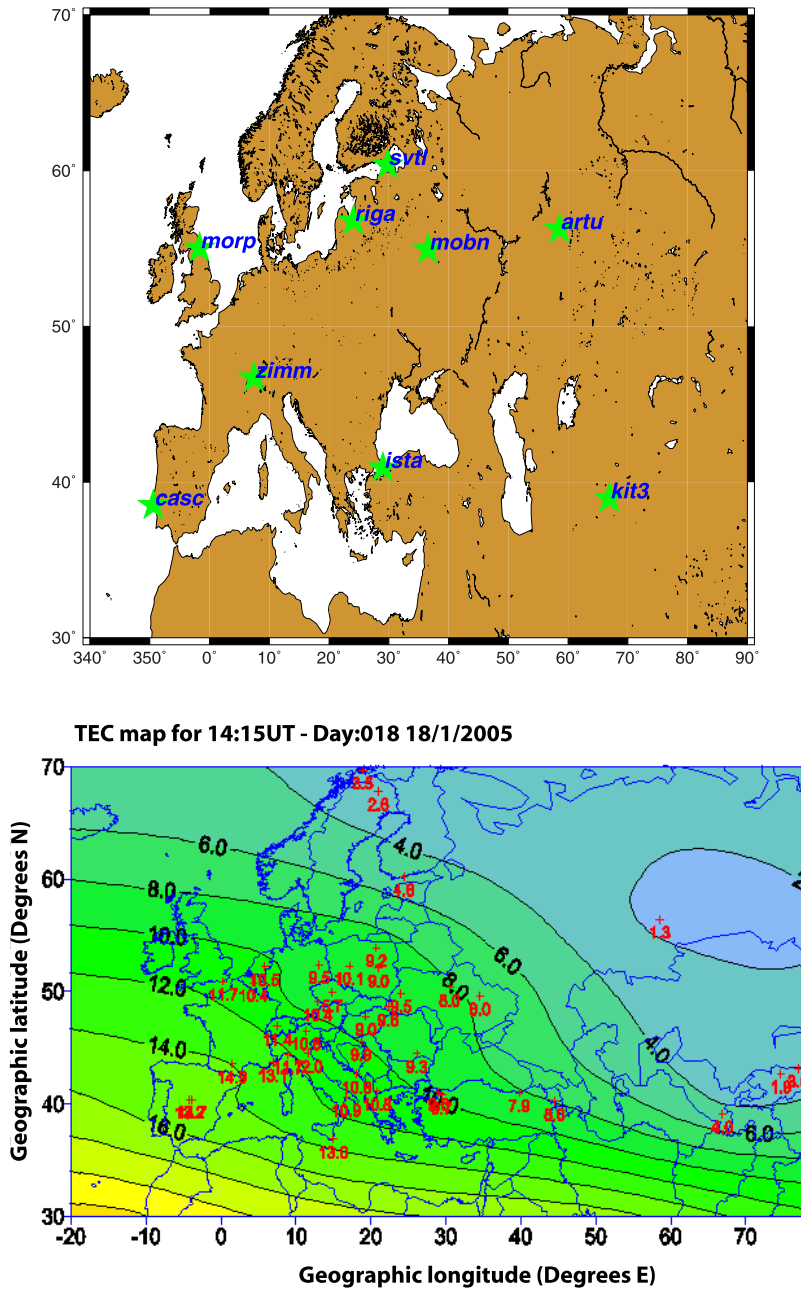


**Figure 5.** (top) Different test stations of the self-consistency test. (bottom) Example of the RAL VTEC map showing the data used to interpolate (red crosses) for 18 January 2005.

stations widely distributed in this stormy week (see top plot of Figure 5). It has to be pointed out that typically the half of the test stations is used in the computation of the RAL maps. However, with such station distribution the  $RMS_{self}$  over each receiver are studied as a function of the zone. This can be useful in order to determine if the interpolation method is accurate, as a

first glance, in regions with low density of GPS observations. Moreover, this network is representative enough in order to compute the mean value of the  $RMS_{self}$  for the whole zone and day for the IGS, UPC and RAL maps. The average results ( $RMS_{self}$ ) are summarized in Table 2. [16] It can be seen in Table 2 that the  $RMS_{self}$  for RAL VTEC is, in general, higher than the corresponding to the

**Table 2.** Self-Consistency Test Results for the Week 15–21 January 2005<sup>a</sup>

	Day of January 2005						
	15	16	17	18	19	20	21
IGS	2.8	2.7	4.3	4.7	2.9	2.6	4.2
UPC	3.0	3.1	5.0	6.0	3.4	2.9	4.6
RAL	3.7	4.3	4.8	4.9	3.5	3.4	5.8

<sup>a</sup>Values are given in TECU.

IGS and UPC ones, as it can be also seen in Figure 6. This is due to the receivers located at edge of the map, and mostly in high latitudes. These errors could indicate (taking into account that the RAL maps have a sampling interval of 10 min) that the interpolation method is not accurate enough to get the local features on the edge of the map (mostly extrapolation). However, since the GIMs cover the whole ionosphere, they do not have edges in those zones and as a consequence there is no degradation due to “edge effect” of the interpolation method.

### 3.2. Jason Altimeter Test

[17] This test is employed to test the different ionospheric maps with independent measure of the vertical TEC over its footprint provided by the altimeter on board the Jason-1 satellite at a mean height orbit of about 1330 km over the Earth’s surface (see *Orus et al.* [2003] for details) characterized by the mean error (bias), RMS and standard deviation regarding to the Jason VTEC as reference.

[18] One of the main features of the Jason-1 ionospheric data is that is gathered over the oceans and seas (see Figure 7 for the footprints over the European region). This feature causes the interpolation method be tested in zones where there are no GPS stations that could take measures. Then, in the European region this data is mostly taken over the Mediterranean Sea (relatively well surrounded by GPS receivers) and the Atlantic Ocean (zone in the edge of VTEC ionospheric map). Thus it is expected that the performance of the Atlantic zone would be worse than the Mediterranean one because of the lack of nearby GPS receivers. However, because of the small amount of data over Europe, the performance values are taken computing the average of the whole data. The daily results for the Jason test are showed in Table 3.

[19] As can be seen in Table 3, there is a significant bias difference of about 1–2 TECUs between the IGS GIMs and the RAL VTEC maps. This bias is especially important on the highest-activity days, reaching a maximum difference of more than 3 TECU. However, the standard deviation is

slightly higher than the IGS GIMs ones but it is quite compatible with them. These results may be due to the fact that the Jason measurements, as it was commented above, are far from the GPS data available, and in the case of the RAL maps, the computation is mostly extrapolation in those areas (see Figure 7, bottom plot, for an example).

## 4. Recomputing VTEC Regional Ionospheric Maps

[20] Kriging technique performs in general a more optimal interpolation, compared with other existing techniques, because it properly addresses the error decorrelation [see *Orus et al.*, 2005]. This is the case, especially when two circumstances meet: There are enough data (1) to interpolate (such STEC values can be obtained in our problems thanks to the VTEC model alignment) and (2) to suffer (the input STECs in our case) a significant model error, this fact being more likely, for instance, in geomagnetic stormy conditions, considered in this paper.

### 4.1. Obtaining High-Sampling Temporal VTEC From $L_I$ Using VTEC Maps

[21] In order to get direct STEC (and VTEC) measurements from a set of dual-frequency carrier phase measurements, from any GPS receiver, a reference global VTEC can be used to level the geometry-free combination of carrier phases. Indeed, the alignment of the ionospheric carrier phase combination with a previously computed STEC (from a file provided for instance in IONEX format) has the advantage of avoiding the local errors affecting the pseudorange measurements, like the multipath, which produces significant errors in the pseudorange alignment procedure [see, e.g., *Ciraolo et al.*, 2006]. In particular, this method allows increasing the ionospheric temporal TEC resolution, for instance 30 s as in the RINEX files, in a simple way. In this context, the VTEC maps are employed to align the geometry free or ionospheric combination  $L_I$  (see equation (2)) to compute the ambiguity term ( $B_I$ ) for each satellite-receiver arc:

$$L_I = STEC + B_I \quad (2)$$

Then, in order to compute the corresponding phase ambiguity for each satellite-receiver continuous arc, the STEC prediction of the VTEC map ( $STEC_{VTEC}$ ) is computed over each satellite ionospheric pierce point (IPP), and then the average is computed as follows:

$$\langle B_I \rangle_i^{j\alpha} = \langle L_{I_i}^{j\alpha} - STEC_{VTEC_i}^{j\alpha} \rangle \quad (3)$$

**Figure 6.** Self-consistency test RMS as a function of the elevation of the satellites in view for different test receivers on 19 January 2005: (a) ARTI, (b) KITAB, and (c) MORPETH.

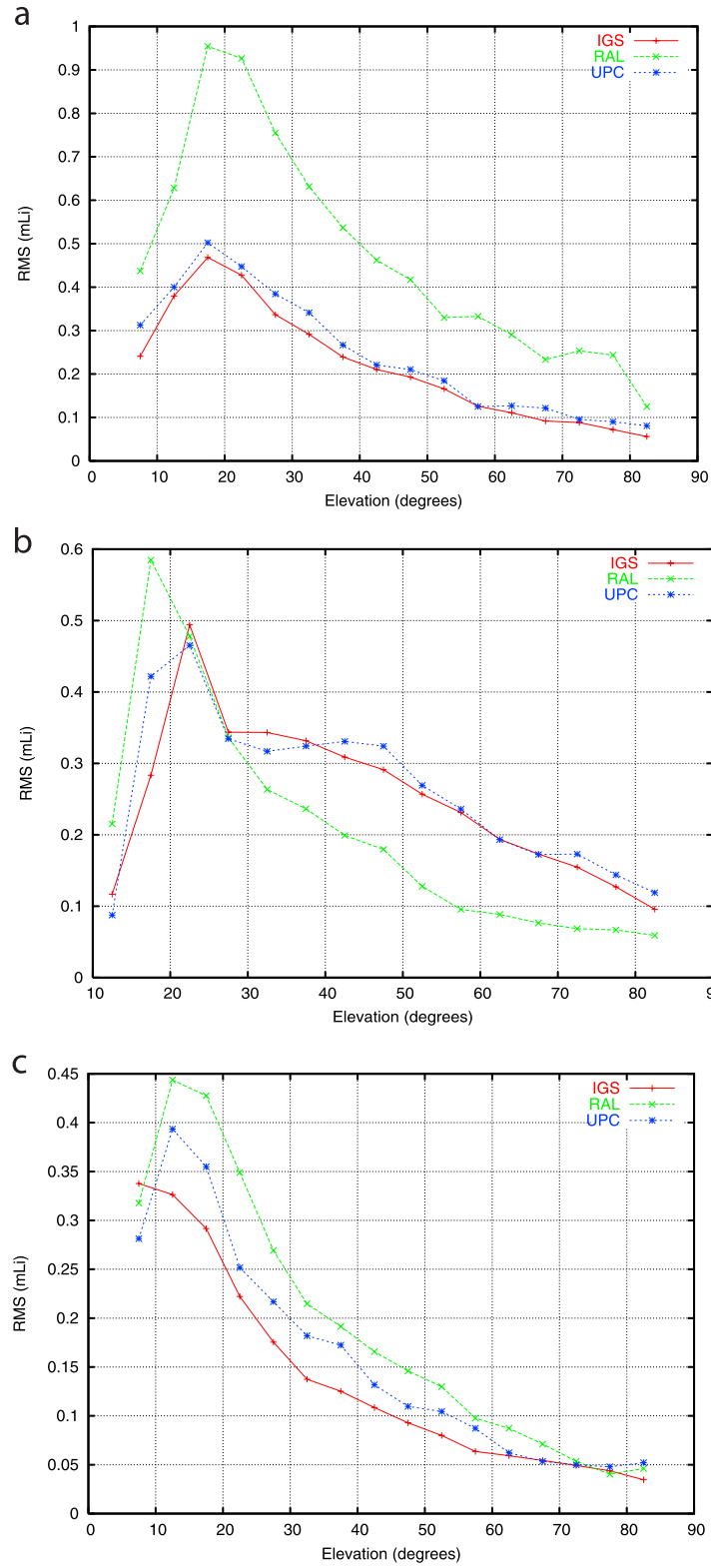
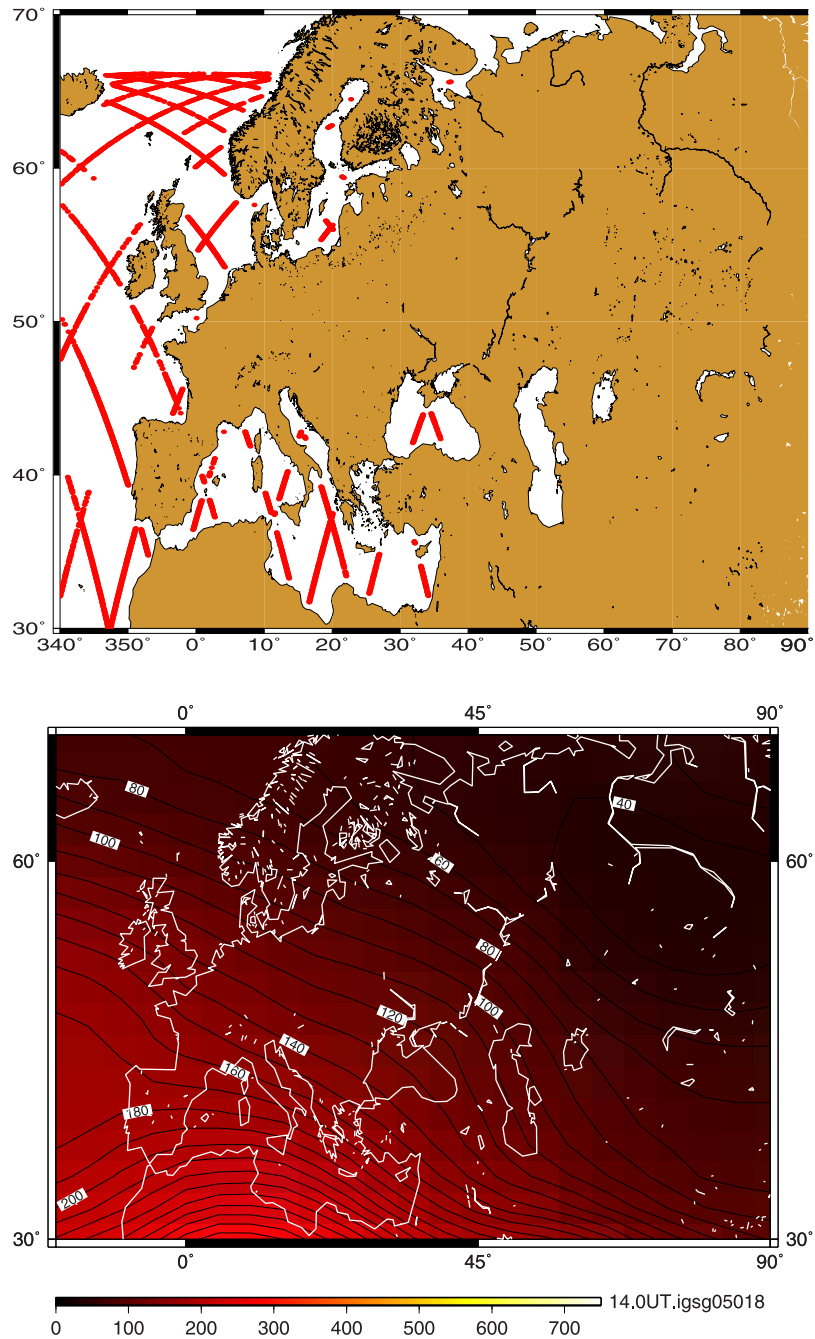


Figure 6



**Figure 7.** (top) Different Jason-1 footprint in the European region. (bottom) Example of the IGS VTEC map showing the data used to interpolate for 18 January 2005.

**Table 3.** Jason Altimeter Test Bias ( $Bias_{Jason}$ ) and Standard Deviation ( $\sigma_{Jason}$ ) for the Week 15–21 January 2005<sup>a</sup>

	Day of January 2005						
	15	16	17	18	19	20	21
IGS	0.7 (1.7)	1.1 (2.0)	2.7 (4.0)	0.7 (3.4)	2.9 (2.3)	2.4 (2.5)	1.0 (2.7)
UPC	0.9 (1.7)	1.4 (2.2)	2.8 (4.2)	0.4 (3.2)	2.9 (2.2)	2.4 (2.4)	1.0 (2.4)
RAL	2.0 (2.4)	1.9 (2.5)	5.1 (4.9)	3.7 (2.7)	4.4 (2.6)	3.6 (2.6)	2.2 (3.0)

<sup>a</sup>Values are given in TECU. Standard deviations are given in parentheses.

where the indices  $i, j$  and  $\alpha$  correspond to the receiver, satellite and arc indicator, and the average is performed over the corresponding continuous (no cycle slips) arc ( $\alpha$ ) of data. With this estimation, the aligned STEC can be obtained:

$$STEC_{align_i}^{j\alpha} = L_{fi}^{j\alpha} - \langle B_I \rangle_i^{j\alpha} \quad (4)$$

and the derived vertical TEC

$$TEC_{align} = STEC_{align_i}^{j\alpha} \cdot F_{IPP}^{-1} \quad (5)$$

where  $F_{IPP}$  is, for example, a typical thin layer mapping function described by

$$F_{IPP}(\varepsilon) = \frac{1}{\sqrt{1 - \left( \frac{R_E}{R_E + h_{ion}} \cos(\varepsilon) \right)^2}} \quad (6)$$

where  $\varepsilon$  is the elevation between the local receiver horizon and satellite line of sight (LOS),  $h_{ion}$  the height of the thin layer, for instance 450 km, and  $R_E$  is the Earth's radius.

[22] Therefore a “leveled” VTEC, with the low temporal resolution (instead of with the code), can be obtained over each IPP each 30 s. Then, the following step is to compute the mean values over the station each 10 min in order to get the input data that will be used to generate the VTEC maps (see Figure 8).

#### 4.2. Using Kriging to Improve the RAL VTEC Maps

[23] Once we have been able to generate RAL model aligned VTEC, we proceed to improve its performance. As it has been shown before the RAL VTEC present higher error, in general, than the IGS VTEC. One way to correct and improve such VTEC maps is to apply the kriging technique; such is indicated by *Orus et al.* [2005]. To do that we need the RAL-like STEC values, computed by the corresponding RAL VTEC model

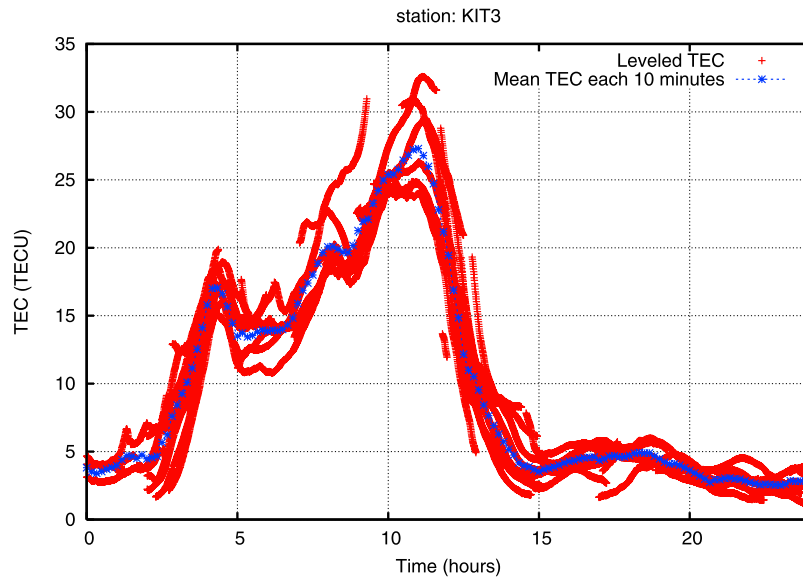


**Figure 8.** Plot showing the leveled raw and the mean VTEC over the station KITAB on 18 January 2005.

**Table 4.**  $\text{RMS}_{\text{self}}$  of the Self-Consistency Test and  $\sigma_{\text{Jason}}$  of the Jason-1 Altimeter Test for the Different RAL VTEC Maps for the Week 15–21 January 2005<sup>a</sup>

	Day of January 2005						
	15	16	17	18	19	20	21
	<i>Self-Consistency Test</i>						
RAL	3.7	4.3	4.8	4.9	3.5	3.4	5.8
RAL Kr.	3.4 (8%)	3.4 (20%)	4.6 (4%)	4.1 (16%)	3.1 (11%)	2.9 (15%)	4.9 (16%)
	<i>Jason-1 Test</i>						
RAL	2.4	2.5	4.9	2.7	2.6	2.6	3.0
RAL Kr.	2.3 (4%)	2.2 (12%)	3.6 (27%)	2.1 (22%)	2.6 (0%)	2.2 (15%)	2.3 (23%)

<sup>a</sup>Values are given in TECU. RAL Kr. Is the kriging technique; relative improvements are shown in parentheses.

alignment, as it has been described above. Such values can be interpolated by kriging, taking into account the residual decorrelation in the interpolation process.

[24] In this study a set of about 40 stations wide distributed over Europe has been used to recompute the RAL VTEC map jointly with the use of the kriging interpolation technique (see *Samardjiev et al.* [1993] and *Orus et al.* [2005] for details). This interpolation technique has the feature that can take into account the spatial correlation between the data use to interpolate. The input data, as has been explained above, is the “leveled” VTEC with the RAL, using the same RINEX files of the IGS stations.

[25] It is also interesting to mention that the number of stations used to recompute the RAL maps are less than the former RAL maps, in fact the original maps are computed with at least 54 stations. The main difference is in the center of Europe, where the density of stations has been reduced in order to decrease the computational load because of redundant data.

[26] The significantly improved results obtained under the self consistency and Jason-1 tests, for the same period of time, are summarized in Table 4. These results suggest that the use of a “leveled” VTEC combined with an improved kriging technique could improve the VTEC maps in stormy conditions.

## 5. Conclusions

[27] A strong space weather conditions scenario has been studied over the European region where the geomagnetic storm starting on 17 January 2005 was an excellent source of data. First, the ionospheric response to this geomagnetic storm has been analyzed using ionosonde and GPS ionospheric data. Then, the feasibility of using the IGS global tests in order to calibrate regional VTEC ionospheric maps has been shown during the stormy conditions for the whole week 15–21 January 2005. Under these conditions the RAL VTEC maps have

been tested showing significant discrepancies, of about several TECU in the Jason test, when it is compared with the official IGS global ionospheric maps (GIM). These discrepancies are more important in the most active days, reaching a difference in the bias of about 3 TECU. However, when the comparison is done using the self-consistency test, which gives a relative confidence of the method, the results are basically compatible, even the RAL maps have RMS values generally higher than the IGS ones.

[28] More importantly, a kriging technique, jointly with a leveled TEC computed estimating the phase ambiguity bias using the ionospheric maps, has been applied in order to improve the RAL estimations in the same stormy conditions. This interpolation scheme, which takes into account the spatial correlation between the data used to interpolate, has introduced improvements up to more than 20% in both tests, showing performances sometimes even better than the official IGS GIMs.

[29] **Acknowledgments.** This work has been partially supported by Agència de Gestió d’Ajuts Universitaris i de Recerca de la Generalitat de Catalunya (AGAUR) and by ESP-2004-05682-C02-01.

## References

- Beutler, G., M. Rothacher, S. Schaer, T. A. Springer, J. Kouba, and R. E. Neilan (1999), The International GPS Service (IGS): An interdisciplinary service in support of Earth sciences, *Adv. Space Res.*, 23(4), 631–635.
- Cander, L. R., and L. Ciralo (2002), First step towards specification of plasmaspheric-ionospheric conditions over Europe on-line, *Acta Geod. Geophys. Hung.*, 37(2–3), 153–161.
- Cander, L. R., and S. J. Mihajlovic (2005), Ionospheric spatial and temporal variations during the 29–31 October 2003 storm, *J. Atmos. Sol. Terr. Phys.*, 67, 1118–1128.

- Cander, L. R., R. Bamford, and J. G. Hickford (2003), Now-casting and forecasting the  $f_oF_2$ , MUF [3000] $F_2$  and TEC based on empirical models and real-time data, in *Twelfth International Conference on Antennas and Propagation (ICAP 2003)*, *IEE Conf. Proc.*, 491(1), 139–142.
- Ciraolo, L., and P. Spalla (1997), Comparison of total electron content from the Navy Navigation Satellite System and the GPS, *Radio Sci.*, 32, 1071–1080.
- Ciraolo, L., F. Azpilicueta, C. Brinini, A. Meza, and S. M. Radicella (2006), Calibration errors on experimental slant total electron content (TEC) determined with GPS, *J. Geod.*, 2, 111–120, doi:10.1007-s00190-006-0093-1.
- Feltens, J., and S. Schaer (1998), IGS products for the ionosphere, paper presented at IGS Analysis Centre Workshop, Eur. Space Oper. Cent., Eur. Space Agency, Darmstadt, Germany.
- Garcia-Rigo, A., M. Hernández-Pajares, J. M. Zornoza, and J. Subirana (2007), Solar flare detection system based on Global Positioning System data. First results, *Adv. Space Res.*, in press.
- Hernández-Pajares, M., J. M. Zornoza, J. Subirana, R. Farnworth, and S. Soley (2005), EGNOS test bed ionospheric corrections under the October and November 2003 storms, *IEEE Trans. Geosci. Remote Sens.*, 43(10), 2283–2293.
- Jakowski, N. (1998), Generation of TEC maps over the COST251 area based on GPS measurements, paper presented at 2nd COST 251 Workshop, Eur. Coop. in the Field of Sci. and Technol., Side, Turkey.
- Liu, H., and H. Lühr (2005), Strong disturbance of the upper thermospheric density due to magnetic storms: CHAMP observations, *J. Geophys. Res.*, 110, A09S29, doi:10.1029/2004JA010908.
- Mannucci, A. J., B. T. Tsurutani, B. A. Iijima, A. Komjathy, A. Saito, W. D. Gonzalez, F. L. Guarnieri, J. U. Kozyra, and R. Skoug (2005), Dayside global ionospheric response to the major interplanetary events of October 29–30, 2003 “Halloween storms,” *Geophys. Res. Lett.*, 32, L12S02, doi:10.1029/2004GL021467.
- Meier, R. R., G. Crowley, D. J. Strickland, A. B. Christensen, L. J. Paxton, D. Morrison, and C. L. Hackert (2005), First look at the 20 November 2003 superstorm with TIMED/GUVI: Comparisons with a thermospheric global circulation model, *J. Geophys. Res.*, 110, A09S41, doi:10.1029/2004JA010990.
- Orus, R., M. Hernandez-Pajares, J. M. Juan, J. Sanz, and M. Garcia-Fernandez (2003), Validation of the GPS TEC maps with TOPEX data, *Adv. Space Res.*, 31(3), 621–627.
- Orus, R., M. Hernandez-Pajares, J. M. Juan, and J. Sanz (2005), Improvement of global ionospheric VTEC maps by using kriging interpolation technique, *J. Atmos. Sol. Terr. Phys.*, 67, 1598–1609.
- Samardjiev, T., P. A. Bradley, L. R. Cander, and M. I. Dick (1993), Ionospheric mapping by computer contouring techniques, *Electron. Lett.*, 29(20), 1794–1975.
- Zolesi, B. (2004), Final report, COST271 action on effects of the upper atmosphere on terrestrial and Earth-space communications, *Ann. Geophys.*, 47, 20–21.

---

L. R. Cander, Rutherford Appleton Laboratory, Chilton OX11 0QX, UK.

M. Hernandez-Pajares, Research Group of Astronomy and Geomatics, Universitat Politècnica de Catalunya, Barcelona E-08034, Spain.

R. Orus, Wave Interaction and Propagation Section, ESTEC, ESA, NL-2200 AG Noordwijk, Netherlands. (raul.orus.perez@esa.int)